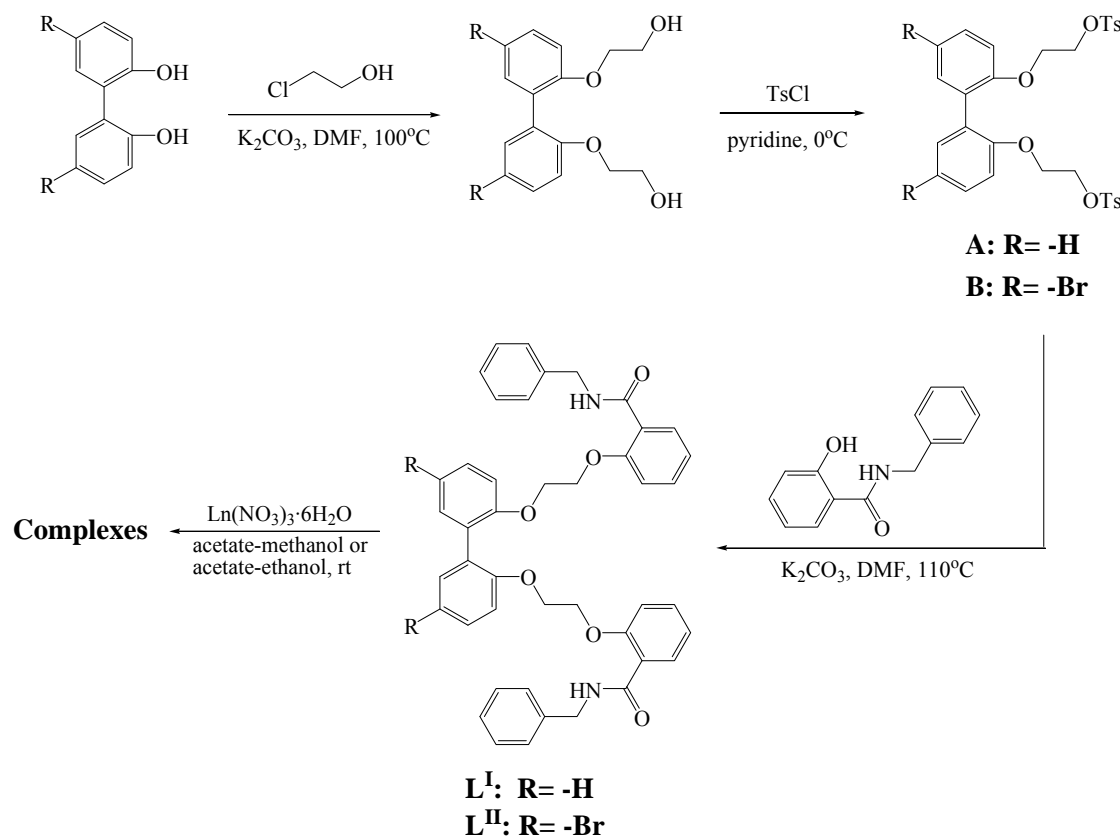

Supporting Information:

Materials and instrumentation

The commercially available chemicals were used without further purification. All of the solvents used were of analytical reagent grade. Lanthanide nitrates¹ and N-benzylsalicylamine² were prepared according to the literature methods, respectively. The intermediates A and B were synthesized following the procedure in literature,³ using 2,2'-biphenol and 5,5'-bibromo-2,2'-biphenol,⁴ respectively, as starting materials.

The metal ions were determined by EDTA titration using xylenol orange as indicator. C, N and H were determined using an Elementar Vario EL. Melting points were determined on a Kofler apparatus. X-Ray powder diffraction (XRPD) patterns were obtained on a Rigaku D/Max-II X-ray diffractometer with graphite-monochromatized Cu-K α radiation. IR spectra were recorded on a Nicolet FT-170SX instrument using KBr discs in the 400–4000 cm⁻¹ region. ¹H NMR spectra were measured on a Bruker DRX 300 spectrometer in CDCl₃ solution with tetramethylsilane as internal standard. Mass spectra were recorded on a Bruker Daltonics esquire6000 Mass spectrometer. UV absorption spectra from 200 to 400 nm were recorded at room temperature on a Varian Cary 100 spectrophotometer in acetonitrile solution using quartz cells of 1.0 cm path length. Fluorescence measurements were made on a Hitachi F-4500 spectrophotometer and a shimadzu RF-540 spectrofluorophotometer equipped with quartz cuvettes of 1 cm path length with a xenon lamp as the excitation source. An excitation and emission slit of 2.5 nm or 1 nm were used for the measurements in the solid state. The 77 K solution-state phosphorescence spectra were recorded with solution samples loaded in a quartz tube inside a quartz-walled optical Dewar flask filled with liquid nitrogen in the phosphorescence mode. Quantum yields were determined by an absolute method using an integrating sphere on FLS920 of Edinburgh Instrument. The luminescence decays were recorded using a pumped dye laser (Lambda Physics model FL2002) as the excitation source. The nominal pulse width and the linewidth of the dye-laser output were 10 ns and 0.18 cm⁻¹, respectively. The emission of a sample was collected by two lenses into a monochromator (WDG30), detected by a photomultiplier and processed by a Boxcar Average (EGG model 162) in line

with a microcomputer. Reported luminescence lifetimes are averages of at least three independent determinations.



Scheme S1 Synthetic procedure for L^I, L^{II} and their lanthanide complexes.

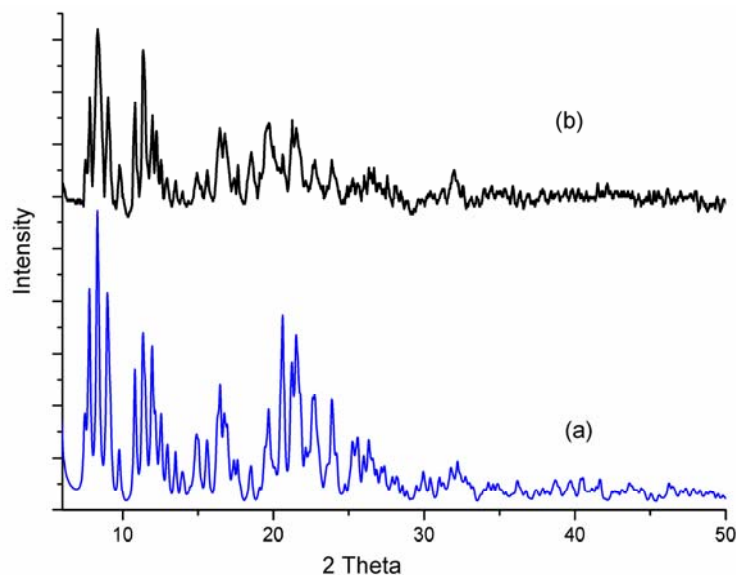


Fig. S1 XRPD patterns of lanthanide complex of ligand L^I (a) simulated for **1**; (b) as-synthesized of Tb³⁺ complex of ligand L^I.

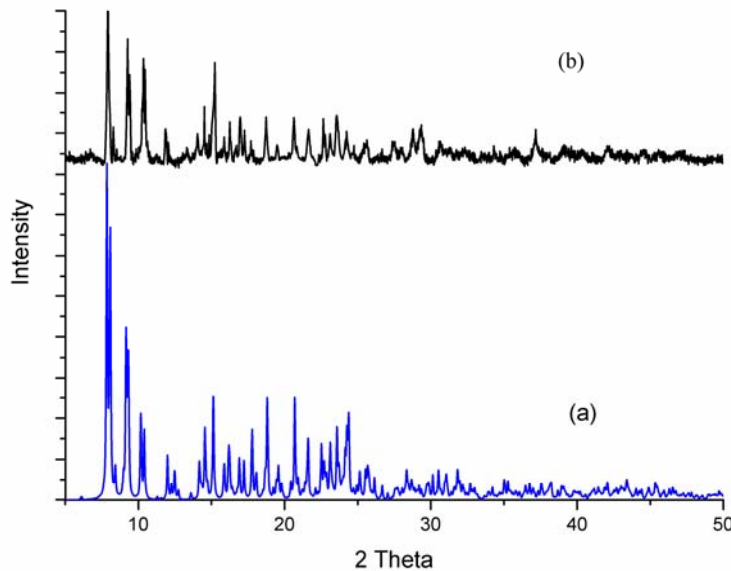


Fig. S2 XRPD patterns of lanthanide complex of ligand L^{II} (a) simulated for **2**; (b) as-synthesized of Dy³⁺ complex of ligand L^{II}.

Absorption Spectra of Ligands.

As shown in Fig. 4, the absorption spectrum of the ligand L^I in acetonitrile features two main bands in the UV region with apparent maxima at ca. 251 ($\varepsilon \sim 10811 \text{ L mol}^{-1} \text{ cm}^{-1}$) and 282 nm ($\varepsilon \sim 11\,714 \text{ L mol}^{-1} \text{ cm}^{-1}$) which can be assigned to characteristic $\pi-\pi^*$ -based transitions centered on the biphenyl and the salicylamide groups, respectively. It is interesting to note that the UV-vis absorption spectrum of L^{II} in acetonitrile is essentially identical to that observed for L^I. The apparent maximum of L^{II} at ca. 252 ($\varepsilon \sim 10099 \text{ L mol}^{-1} \text{ cm}^{-1}$) shows that the substitution of the biphenyl backbone does not have a significant influence on the electronic properties of the biphenyl group due to cooperative effects of the weak

electron-pulling character and the bromine lone pair induced $n-\pi^*$ back-energy transiton character of the bromine fragment. However, a small red shift observed in the absorption maximum of L^{II} (apparent maximum at ca. 287 nm ($\varepsilon \sim 10484 \text{ L mol}^{-1} \text{ cm}^{-1}$)) may be a consequence of the transition of the salicylamide groups with mixed $n-\pi^*$, $\pi-\pi^*$ parentage.⁵ We note that molar absorption coefficients at the maxima of the bands for the ligands are large, indicates that the two ligands have a strong ability to absorb light and thus favor efficient antenna effect, making them possible candidates as activators for lanthanide luminescence.

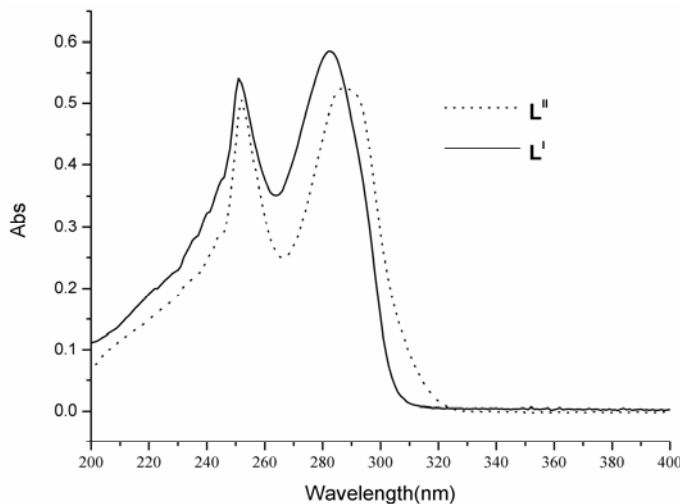


Fig. S3 Absorption spectra of L^I (solid line) and L^{II} (dotted line) in acetonitrile ($5 \times 10^{-5} \text{ M}$).

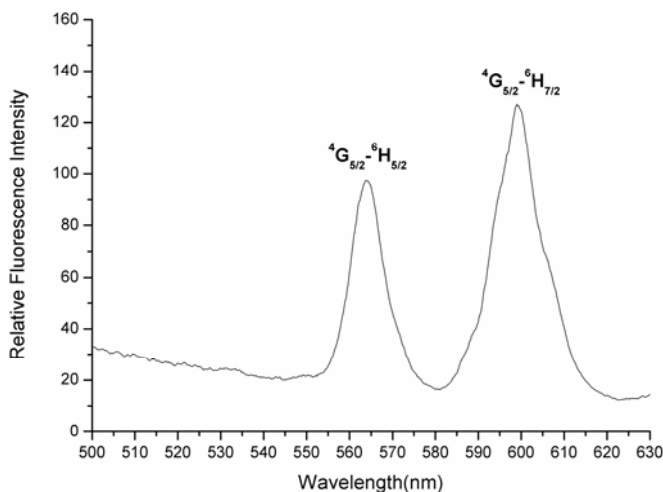


Fig. S4 Room-temperature emission spectrum for Sm^{3+} complex of ligand L^I excited at 317 nm (excitation and emission passes = 2.5 nm).

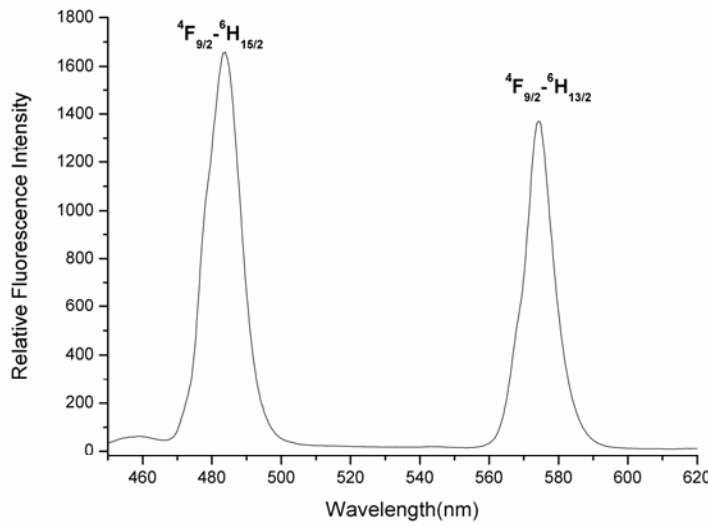


Fig. S5 Room-temperature emission spectrum for Dy^{3+} complex of ligand L^1 excited at 317 nm (excitation and emission passes = 2.5 nm).

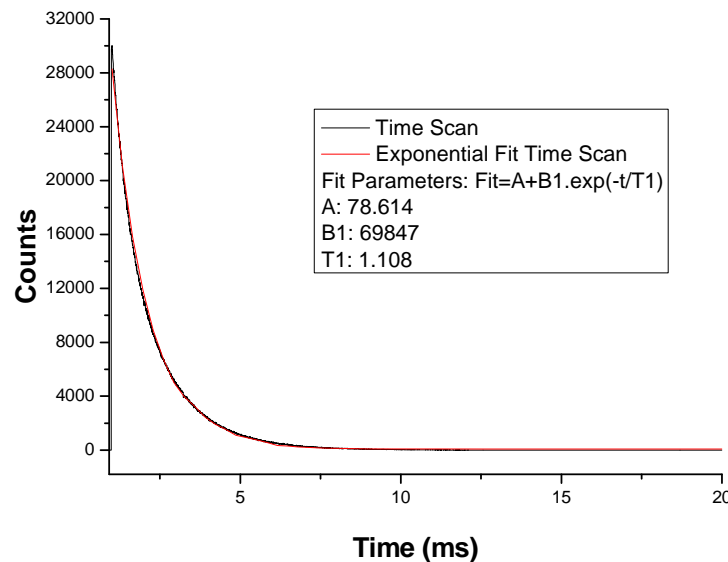


Fig. S6 The room-temperature solid-state phosphorescence lifetime of Eu^{3+} complex of ligand L^1 .

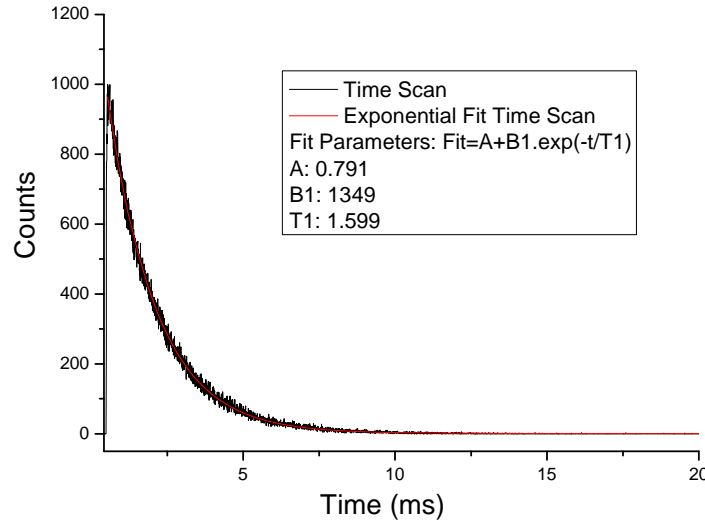


Fig. S7 The room-temperature solid-state phosphorescence lifetime of Tb^{3+} complex of ligand L^{I} .

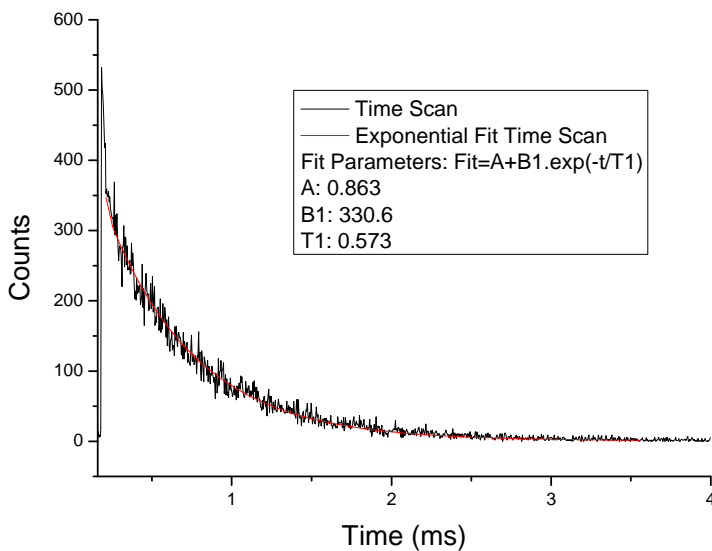


Fig. S8 The room-temperature solid-state phosphorescence lifetime of Eu^{3+} complex of ligand L^{II} .

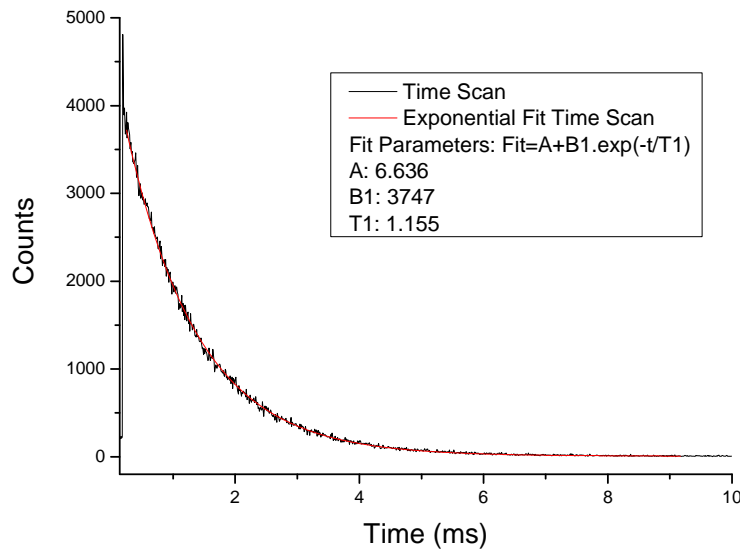


Fig. S9 The room-temperature solid-state phosphorescence lifetime of Tb^{3+} complex of ligand L^{II} .

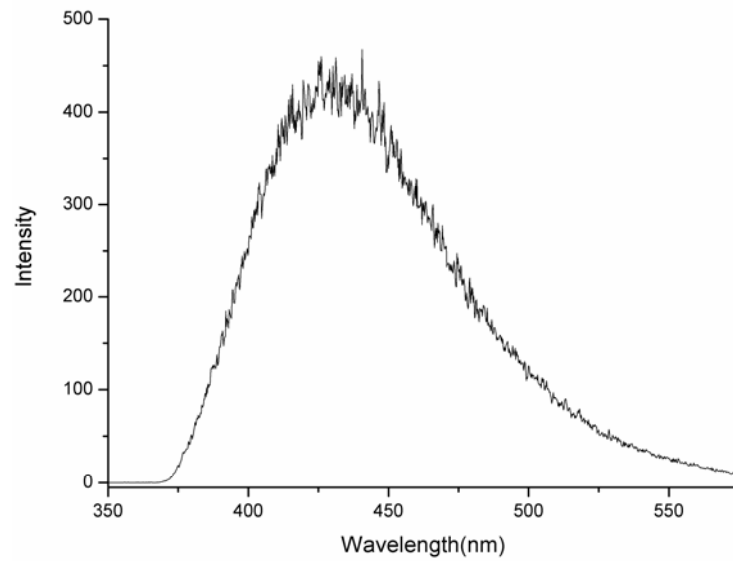


Fig. S10 Phosphorescence spectrum of Gd^{3+} complex of ligand L^{I} excited at 302 nm at 77K.

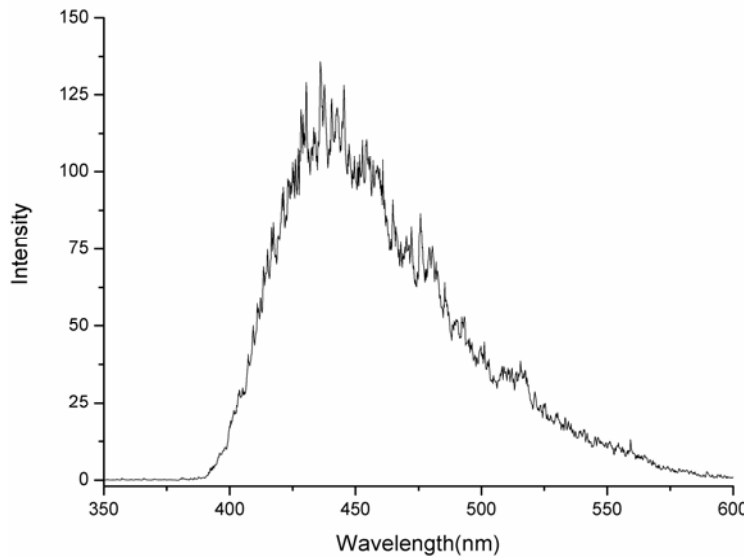


Fig. S11 Phosphorescence spectrum of Gd^{3+} complex of ligand L^{II} excited at 310 nm at 77K.

Table S1. Selected bond distances (\AA) and angles ($^\circ$) for polymer **1**

Nd(1)-O(18)#1	2.375(5)	Nd(1)-O(13)	2.396(5)	Nd(1)-O(3)	2.412(5)	Nd(1)-O(10)	2.524(5)
Nd(1)-O(5)	2.529(6)	Nd(1)-O(8)	2.530(5)	Nd(1)-O(4)	2.531(5)	Nd(1)-O(7)	2.537(5)
Nd(1)-O(12)	2.562(5)						
O(18)#1-Nd(1)-O(13)	84.70(19)	O(3)-Nd(1)-O(8)	118.9(2)	O(10)-Nd(1)-O(7)	120.48(19)		
O(18)#1-Nd(1)-O(3)	87.49(18)	O(10)-Nd(1)-O(8)	75.33(19)	O(5)-Nd(1)-O(7)	71.73(19)		
O(13)-Nd(1)-O(3)	89.92(18)	O(5)-Nd(1)-O(8)	71.38(19)	O(8)-Nd(1)-O(7)	49.9(2)		
O(18)#1-Nd(1)-O(10)	86.42(18)	O(18)#1-Nd(1)-O(4)	71.7(2)	O(4)-Nd(1)-O(7)	115.3(2)		
O(13)-Nd(1)-O(10)	120.55(19)	O(13)-Nd(1)-O(4)	154.65(19)	O(18)#1-Nd(1)-O(12)	82.60(18)		
O(3)-Nd(1)-O(10)	148.1(2)	O(3)-Nd(1)-O(4)	80.27(18)	O(13)-Nd(1)-O(12)	70.24(18)		
O(18)#1-Nd(1)-O(5)	121.9(2)	O(10)-Nd(1)-O(4)	68.11(19)	O(3)-Nd(1)-O(12)	158.49(19)		
O(13)-Nd(1)-O(5)	153.00(19)	O(5)-Nd(1)-O(4)	50.43(19)	O(10)-Nd(1)-O(12)	50.33(19)		
O(3)-Nd(1)-O(5)	87.05(19)	O(8)-Nd(1)-O(4)	118.4(2)	O(5)-Nd(1)-O(12)	114.39(18)		
O(10)-Nd(1)-O(5)	70.0(2)	O(18)#1-Nd(1)-O(7)	153.08(19)	O(8)-Nd(1)-O(12)	69.7(2)		

O(18)#1-Nd(1)-O(8) 152.3(2)	O(13)-Nd(1)-O(7) 82.12(19)	O(4)-Nd(1)-O(12) 114.16(18)
O(13)-Nd(1)-O(8) 86.83(18)	O(3)-Nd(1)-O(7) 69.18(19)	O(7)-Nd(1)-O(12) 114.38(19)

Symmetry transformations used to generate equivalent atoms: #1 = -x+1/2, y-1/2, -z+1/2

Table S2. Selected bond distances (\AA) and angles ($^{\circ}$) for polymer **2**

Nd(1)-O(6) 2.371(7)	Nd(1)-O(1)#1 2.399(7)	Nd(1)-O(16) 2.493(7)	Nd(1)-O(10) 2.510(8)
Nd(1)-O(15) 2.524(8)	Nd(1)-O(12) 2.526(8)	Nd(1)-O(9) 2.563(7)	Nd(1)-O(7) 2.586(6)
Nd(1)-O(13) 2.615(9)			
O(6)-Nd(1)-O(1)#1 85.0(2)	O(16)-Nd(1)-O(12) 76.8(3)	O(10)-Nd(1)-O(7) 115.0(3)	
O(6)-Nd(1)-O(16) 84.5(2)	O(10)-Nd(1)-O(12) 50.9(3)	O(15)-Nd(1)-O(7) 156.5(3)	
O(1)#1-Nd(1)-O(16) 152.5(2)	O(15)-Nd(1)-O(12) 84.2(3)	O(12)-Nd(1)-O(7) 119.2(3)	
O(6)-Nd(1)-O(10) 151.3(3)	O(6)-Nd(1)-O(9) 124.9(2)	O(9)-Nd(1)-O(7) 49.8(2)	
O(1)#1-Nd(1)-O(10) 70.8(3)	O(1)#1-Nd(1)-O(9) 87.5(2)	O(6)-Nd(1)-O(13) 76.1(3)	
O(16)-Nd(1)-O(10) 124.0(3)	O(16)-Nd(1)-O(9) 78.0(3)	O(1)#1-Nd(1)-O(13) 129.8(3)	
O(6)-Nd(1)-O(15) 85.7(3)	O(10)-Nd(1)-O(9) 70.6(3)	O(16)-Nd(1)-O(13) 71.5(3)	
O(1)#1-Nd(1)-O(15) 83.0(3)	O(15)-Nd(1)-O(9) 147.1(3)	O(10)-Nd(1)-O(13) 107.4(3)	
O(16)-Nd(1)-O(15) 121.3(3)	O(12)-Nd(1)-O(9) 74.2(3)	O(15)-Nd(1)-O(13) 50.0(3)	
O(10)-Nd(1)-O(15) 76.5(3)	O(6)-Nd(1)-O(7) 75.1(3)	O(12)-Nd(1)-O(13) 75.6(3)	
O(6)-Nd(1)-O(12) 149.8(3)	O(1)#1-Nd(1)-O(7) 82.0(2)	O(9)-Nd(1)-O(13) 141.0(3)	
O(1)#1-Nd(1)-O(12) 121.7(3)	O(16)-Nd(1)-O(7) 70.8(2)	O(7)-Nd(1)-O(13) 134.0(3)	

Symmetry transformations used to generate equivalent atoms: #1 = -x+3/2, y-1/2, -z+3/2

Table S3. Selected bond distances (\AA) and angles ($^{\circ}$) for polymer **3**

Eu(1)-O(3) 2.236(16)	Eu(1)-O(5) 2.266(12)	Eu(1)-O(16) 2.374(12)	Eu(1)-O(13) 2.380(13)
Eu(1)-O(14) 2.381(15)	Eu(1)-O(10) 2.391(15)	Eu(1)-O(8) 2.458(12)	Eu(1)-O(7) 2.511(12)
Eu(1)-O(11) 2.513(14)			
O(3)-Eu(1)-O(5) 83.7(4)	O(16)-Eu(1)-O(10) 122.9(5)	O(13)-Eu(1)-O(7) 114.2(4)	
O(3)-Eu(1)-O(16) 86.1(4)	O(13)-Eu(1)-O(10) 76.1(5)	O(14)-Eu(1)-O(7) 121.2(5)	
O(5)-Eu(1)-O(16) 151.4(4)	O(14)-Eu(1)-O(10) 82.7(5)	O(10)-Eu(1)-O(7) 155.8(5)	
O(3)-Eu(1)-O(13) 149.0(5)	O(3)-Eu(1)-O(8) 125.6(5)	O(8)-Eu(1)-O(7) 49.3(4)	
O(5)-Eu(1)-O(13) 70.3(5)	O(5)-Eu(1)-O(8) 87.9(4)	O(3)-Eu(1)-O(11) 76.6(5)	
O(16)-Eu(1)-O(13) 124.7(5)	O(16)-Eu(1)-O(8) 76.5(4)	O(5)-Eu(1)-O(11) 129.2(5)	
O(3)-Eu(1)-O(14) 148.6(5)	O(13)-Eu(1)-O(8) 71.2(5)	O(16)-Eu(1)-O(11) 73.5(5)	
O(5)-Eu(1)-O(14) 122.6(5)	O(14)-Eu(1)-O(8) 76.3(5)	O(13)-Eu(1)-O(11) 106.9(5)	
O(16)-Eu(1)-O(14) 77.2(5)	O(10)-Eu(1)-O(8) 147.3(5)	O(14)-Eu(1)-O(11) 73.3(5)	
O(13)-Eu(1)-O(14) 52.3(5)	O(3)-Eu(1)-O(7) 76.3(5)	O(10)-Eu(1)-O(11) 49.6(5)	

O(3)-Eu(1)-O(10) 84.4(5)	O(5)-Eu(1)-O(7) 80.9(4)	O(8)-Eu(1)-O(11) 141.0(5)
O(5)-Eu(1)-O(10) 82.6(4)	O(16)-Eu(1)-O(7) 70.7(4)	O(7)-Eu(1)-O(11) 136.0(5)

Table S4. Selected bond distances (\AA) and angles ($^{\circ}$) for polymer **4**

Tb(1)-O(3) 2.249(19)	Tb(1)-O(5) 2.309(16)	Tb(1)-O(10) 2.326(16)	Tb(1)-O(16) 2.382(13)
Tb(1)-O(14) 2.427(16)	Tb(1)-O(13) 2.428(17)	Tb(1)-O(7) 2.481(17)	Tb(1)-O(11) 2.489(16)
Tb(1)-O(8) 2.499(16)			
O(3)-Tb(1)-O(5) 85.2(5)	O(10)-Tb(1)-O(13) 75.2(6)	O(16)-Tb(1)-O(11) 71.4(5)	
O(3)-Tb(1)-O(10) 84.1(6)	O(16)-Tb(1)-O(13) 125.7(6)	O(14)-Tb(1)-O(11) 76.2(6)	
O(5)-Tb(1)-O(10) 81.4(5)	O(14)-Tb(1)-O(13) 52.4(5)	O(13)-Tb(1)-O(11) 107.5(6)	
O(3)-Tb(1)-O(16) 84.2(5)	O(3)-Tb(1)-O(7) 77.8(6)	O(7)-Tb(1)-O(11) 134.6(5)	
O(5)-Tb(1)-O(16) 152.5(5)	O(5)-Tb(1)-O(7) 82.3(4)	O(3)-Tb(1)-O(8) 127.6(6)	
O(10)-Tb(1)-O(16) 122.5(5)	O(10)-Tb(1)-O(7) 156.5(5)	O(5)-Tb(1)-O(8) 89.2(5)	
O(3)-Tb(1)-O(14) 148.7(6)	O(16)-Tb(1)-O(7) 70.7(5)	O(10)-Tb(1)-O(8) 146.2(6)	
O(5)-Tb(1)-O(14) 122.5(6)	O(14)-Tb(1)-O(7) 117.2(6)	O(16)-Tb(1)-O(8) 77.5(5)	
O(10)-Tb(1)-O(14) 85.9(6)	O(13)-Tb(1)-O(7) 114.5(5)	O(14)-Tb(1)-O(8) 71.9(6)	
O(16)-Tb(1)-O(14) 76.4(6)	O(3)-Tb(1)-O(11) 74.5(5)	O(13)-Tb(1)-O(8) 71.0(6)	
O(3)-Tb(1)-O(13) 149.6(6)	O(5)-Tb(1)-O(11) 129.3(5)	O(7)-Tb(1)-O(8) 49.9(5)	
O(5)-Tb(1)-O(13) 70.1(5)	O(10)-Tb(1)-O(11) 51.2(5)	O(11)-Tb(1)-O(8) 139.6(5)	

References:

- (1) Nakagawa, K.; Amita, K.; Mizuno, H.; Inoue, Y.; Hakushi, T. *Bull. Chem. Soc. Jpn.* **1987**, *60*, 2037-2040.
- (2) Michio, K. *Bull. Chem. Soc. Jpn.* **1976**, *49*, 2679-2682.
- (3) (a) Huang, Z.; Chen, Y.; Chi, W.; Xu, W.; Zheng, B.; Wei, Y. *Huaxue Shiji* **1995**, *17*, 331-334. (b) Ando, N.; Ohi, S.; Yamamoto, Y.; Oda, J.; Inouye, Y. *Bull. Inst. Chem. Res., Kyoto Univ.* **1980**, *58*, 293-307.
- (4) Facchetti, S.; Losi, D.; Iuliano, A. *Tetrahedron: Asymmetry* **2006**, *17*, 2993–3003.
- (5) Moore, E. G.; Xu, J.; Jocher, C. J.; Castro-Rodriguez, I.; Raymond, K. N. *Inorg. Chem.* **2008**, *47*, 3105-3118.